PRAMANA — journal of physics

Vol. 86, No. 1
January 2016
pp. 127–134

Electronic properties of GaV_4S_8: A percolation approach

I NAIK[1,*], S HANSDA[1] and A K RASTOGI[2]

[1]Department of Physics, North Orissa University, Baripada 757 003, India
[2]School of Physical Sciences, Jawaharlal Nehru University, New Delhi 110 067, India
*Corresponding author. E-mail: indrajit_naik@yahoo.co.in

MS received 28 July 2014; revised 11 October 2014; accepted 27 October 2014
DOI: 10.1007/s12043-015-1014-8; ***e*Publication:** 26 August 2015

Abstract. Two polycrystalline V_4-cluster compounds of GaV_4S_8 were prepared at different annealing temperatures (GaV_4S_8-1 sintered at 800°C and GaV_4S_8-2 sintered at 500°C). Their temperature-dependent resistivity and structural phase transformation temperature (45 K for GaV_4S_8-1 and 43 K for GaV_4S_8-2) are found to be very sensitive to the annealing condition. Above 320 K, activation energy ε_3 is calculated to be ∼0.23 eV which decreases to ∼0.18 eV around 300 K in GaV_4S_8-1 and GaV_4S_8-2 on cooling. According to percolation theory, the gradual decrease in ε_3 below 300 K is expected due to the increase in separation between V_4-clusters are significantly different in GaV_4S_8-1 and GaV_4S_8-2. This statement is strongly supported by the calculated bandwidth Γ per cluster in GaV_4S_8 (∼0.342 eV in GaV_4S_8-1 and ∼0.374 eV in GaV_4S_8-2). A negative magnetoresistance (MR) is also found around 43 K in GaV_4S_8-2 at 6.0 T magnetic field associated with structural transition.

Keywords. Transition metal compound; percolation theory; magnetoresistance.

PACS Nos 72.80.Ga; 64.60.ah; 75.47.Gk

1. Introduction

The electronic properties in AM_4X_8, where M = V, Nb or Ta and X = S, Se or Te, are dominated by strongly correlated electrons and closely related to its peculiar crystal structure of $GaMo_4S_8$ derived from spinel AM_2X_4 as $A_{0.5}\square_{0.5}M_2X_4$ [1,2]. The ordering between A-ions and vacancies (□) on tetrahedral sites in defect spinel i.e., $A_{0.5}\square_{0.5}M_2X_4$ reduces the space group of spinel $Fd3m$ to diamond lattice $F\bar{4}3m$ [3,4]. Thus, $GaMo_4S_8$-type of structure is obtained in GaV_4S_8, the V-ions shift from their usual octahedral position to form tetrahedral V_4-cluster within the cubic units V_4S_4. This structural modification results in intracluster V–V distance in which d electrons form molecular orbitals similar to cluster orbitals that are highly degenerate with one unpaired electron because each V_4-cluster contains seven valence electrons within the ionic configuration $Ga^{3+}V_4^{3.25+}S_8^{2-}$ and the large intercluster distance make correlations among the unpaired

electrons between V_4-clusters responsible for magnetism [5]. The correlation between degenerate orbital electrons in GaV_4S_8 are remarkably different from the electrons in a narrow-band solid, such as V_2O_3, high-temperature superconductors etc., and results in non-metallic magnetic properties represented by Mott insulator. Further, the structure of GaV_4S_8 is also described by arranging $[GaS_4]^{5-}$ ions and $[V_4S_4]^{5+}$ cluster ions as NaCl-type lattice. Besides its structural importance at room temperature, low-temperature properties like hopping conduction [6–8], structural change i.e., 45 K [9–11] and ferromagnetism, i.e., 13 K [5,12] have been reported extensively in GaV_4S_8.

In this paper we have reported the electrical conductivity from 30 to 600 K on two differently sintered pellets. Though the hopping conduction and structural phase transition exist in both the sintered pellets as reported earlier, the low-temperature conductivity and phase transition temperature are different from each other. The difference in the electronic properties on GaV_4S_8 is discussed using percolation model in §3.

2. Theoretical model

In disordered compounds, the process of electrical conduction is different from normal metals and is described either by percolation or hopping of charge carriers between the neighbouring sites. Percolation method, in which charge carriers move between the nearest-neighbour sites connected by bonds of finite resistance is different from hopping method in which charge carriers are localized to a particular site and move to a suitable site by hopping. Though the mechanisms of these two processes are different, their conductivity behaviour is similar. Therefore, the DC conductivity due to the movement of charge carriers between two well-connected sites of m and m' is given by Miller and Abrahams [13] on averaging the random resistor network as follows:

$$Z_{mm'}^{-1} = Z_0^{-1} \mathrm{e}^{-2\alpha|R_{mm'}| - \frac{\beta}{2}(|\varepsilon_{m'}-\mu|+|\varepsilon_m-\mu|+|\varepsilon_{m'}-\varepsilon_m|) \le \zeta}, \tag{1}$$

where $Z_{mm'}$ is the resistance between the sites m and m', $R_{mm'} = R_m - R_{m'}$, where R_m is the position of the mth site in three dimensions with energy ε_m and chemical potential μ. The size of the site is represented by the wave function with Bohr radius α^{-1}. Percolation theory is valid for $R_{mm'} \le R_c$, where R_c is the critical value at which the percolation path opens between the sites in the network and current continues to flow across the network if the separation between the two sites increases from $\zeta_c/2\alpha$, where $\zeta_c = 2\alpha R_c$. In this scenario eq. (1) modifies as

$$\rho = \rho_0 \mathrm{e}^{\zeta_c} \mathrm{e}^{\varepsilon_3/k_B T} = \rho_3 \mathrm{e}^{\varepsilon_3/k_B T}. \tag{2}$$

Here $\varepsilon_3 \approx |\varepsilon_0 - \mu|$ for $\varepsilon_m = \varepsilon_{m'} = \varepsilon_0$ is the activation energy. This expression is the same as that for hopping conduction. The pre-exponential factor ρ_3 depends on either the concentrations of sites (R-percolation) or energy-dependent mutual distance between the sites (R–ε-percolation).

R-percolation. At sufficiently high temperature, the temperature exponent becomes unimportant and the resistance depends only on the distance between the two sites $R_{mm'}$, i.e., $\varepsilon_3/k_B T \ll \alpha/N^{1/3}$. $\zeta_c = 2\alpha R_c = \eta\alpha/N^{1/3}$ implies that $\eta = 2R_c N^{1/3} = 1.289$ is a number of the order of unity calculated from the percolation theory using the value of

Pike and Seager [14] average number of bonds per site ($B_c = 2.7$) in a three-dimensional system of N sites per unit volume. Then the resistivity becomes

$$\rho \approx \rho_3 = \rho_0 e^{\eta\alpha/N^{1/3}}. \tag{3}$$

For percolation process, the average value of $\alpha/N^{1/3}$ must be >4 or 5 which can be obtained from eqs (2) and (3). If $\varepsilon_3 > k_B T$, then the activated temperature dependence in $\rho\,(T)$ is valid. Otherwise, the pre-exponential factor plays a major role in conductivity.

R–ε-percolation. At sufficiently low temperature, the temperature as well as the resistance become important as

$$\frac{|R_{mm'}|}{R_{\max}} + \frac{|\varepsilon_m - \mu| + |\varepsilon_{m'} - \mu| + |\varepsilon_m - \varepsilon_{m'}|}{E_{\max}} \leq 1.$$

Here the value of ζ_c is equal to $\zeta_c + (\varepsilon_3/k_B T)$ and obtained from $\bar{R} = \gamma R_{\max}$ (γ is a number) using $R_{\max} = \zeta/2\alpha$, $E_{\max} = k_B T\zeta$ and $\phi_c = n(4\pi\bar{R}^3/3)$, where $\bar{R}$ is the average radius of the sites and $n = 2N(\varepsilon_F)E_{\max}$ is the concentration of sites.

$$\zeta_c = \left(\frac{3\phi_c\alpha^3}{\pi\gamma^3 N(\varepsilon_F)k_B T}\right)^{1/4} = \left(\frac{T_0}{T}\right)^{1/4},$$

where

$$T_0 = \frac{3\phi_c\alpha^3}{\pi\gamma^3 N(\varepsilon_F)k_B} = \frac{c_3^4\alpha^3}{N(\varepsilon_F)k_B}.$$

Here, $N(\varepsilon_F)$ is the number density of sites at Fermi energy ε_F and c_3 is a numerical constant. Depending on the procedure of averaging the current path c_3 lies between 1.84 and 2.436 [15]. Then the resistivity ρ is obtained by substituting the value of ζ_c in eq. (2)

$$\rho = \rho_0 e^{(T_0/T)^{1/4}}. \tag{4}$$

This expression is similar to the Mott's variable range hopping conduction, which provides information about the energy-dependent Bohr radius from $\alpha/N^{1/3}$.

3. Results and discussion

3.1 *Sample preparation*

In our present study, we have obtained two polycrystalline compounds GaV_4S_8-1 sintered at 800°C for 7 days and GaV_4S_8-2 by re-sintering GaV_4S_8-1 at 500°C for 10 days by solid-state reaction method from pure elements. The better crystalline order is inferred from relatively sharper peaks found in GaV_4S_8-2 compared to GaV_4S_8-1 from room temperature (i.e., 300 K) X-ray diffraction as shown in figure 1 and their cubic lattice constants are calculated as ∼9.665 Å and ∼9.662 Å, respectively similar to that obtained in [9].

In the present scenario of GaV_4S_8 compound, each V_4-cluster represents the site for percolation in the form of V_4S_4 and its Bohr radius is estimated from the percolation

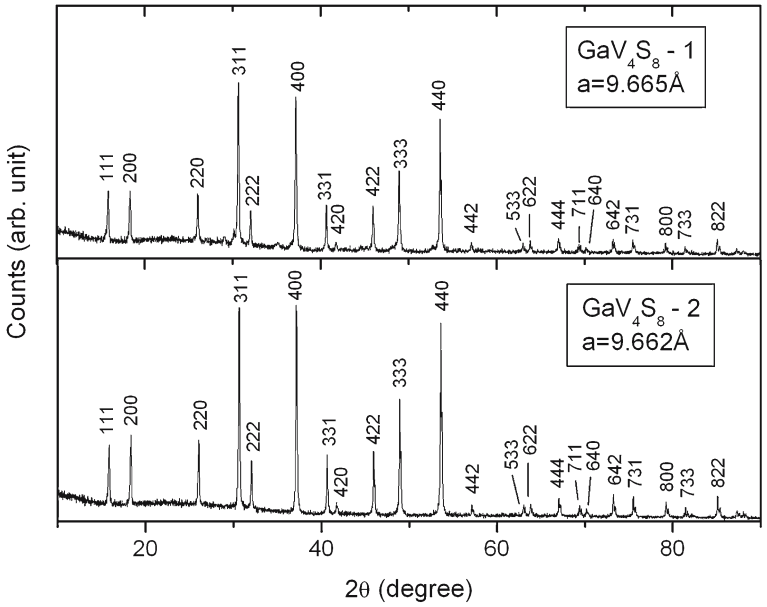

Figure 1. X-ray diffraction of GaV_4S_8-1 and GaV_4S_8-2 at room temperature.

theory. Though there is a slight difference in X-ray diffraction peaks between GaV_4S_8-1 and GaV_4S_8-2, the number density N of V_4-cluster and the number of charge carriers per site in GaV_4S_8 are the same because of the identical chemical composition.

3.2 *Resistivity*

The resistivity of GaV_4S_8 (GaV_4S_8-1 annealed at 800°C and GaV_4S_8-2 annealed at 500°C) are measured by four-probe method of van der Pauw geometry in the temperature range of 30–600 K and plotted as $\log \rho$ vs. $1/T$ using eq. (2) shown in figure 2. The room-temperature resistivity is found to be ∼4.0 Ω cm in both the compounds. Figure 2 also shows that the resistivities in both the compounds are the same above 260 K and below this temperature they behave differently. Therefore, in the following we have discussed the possible mechanism for GaV_4S_8 using percolation theory.

Above 330 K. On cooling from 600 K, the resistivity follows an Arrhenius dependence, $\log \rho \sim 1/T$, showing the same slope in both the compounds and activation energy is estimated to be $\varepsilon_3 \sim 0.23\,\text{eV} > k_\text{B}T$ above 320 K. According to eq. (3), the intercept value ($\log \rho_3$) in $\log \rho$ is found to be equal irrespective of their crystalline disorder indicating identical average Bohr radius (α^{-1}) in both the compounds.

Between 60 *and* 320 K. On cooling, the non-Arrhenius plot on GaV_4S_8 shows different conduction behaviours for compounds annealed differently. A clear changeover of around 260 K is noticed in the inverse temperature dependence of $\log \rho$ (see the inset of figure 2). Below 260 K, the $\log \rho$ vs. $1/T$ shows downward curvature associated with a continuous reduction in the activation energy. However, we have calculated the activation energies

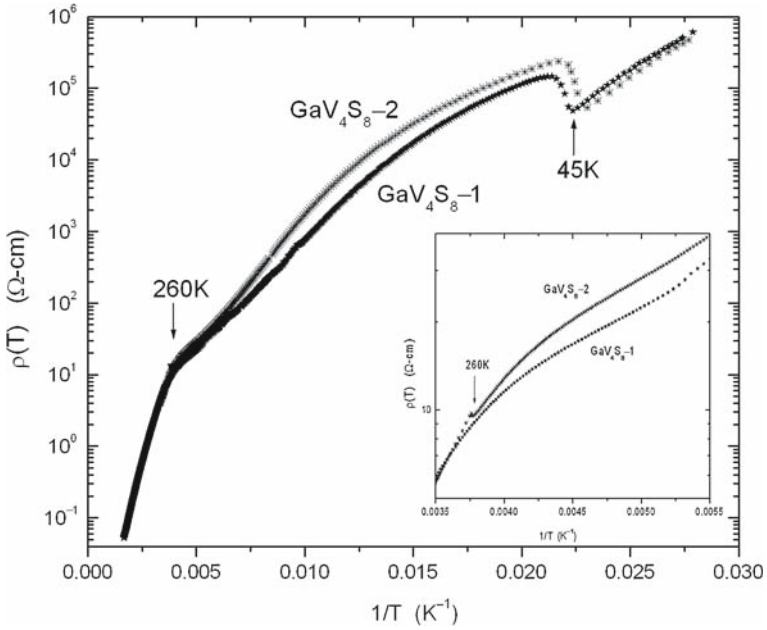

Figure 2. Log ρ vs. $1/T$ plot for GaV_4S_8-1 annealed at 800°C and GaV_4S_8-2 annealed at 500°C. Inset figure shows the change in log ρ around 260 K in GaV_4S_8-1 and GaV_4S_8-2.

at around 300 and 170 K in both the compounds and presented in table 1. The room-temperature activation energies are almost the same as reported in [6,8]. Besides the non-Arrhenius behaviour of GaV_4S_8, the resistivities are well fitted by Mott's law below 170 K in GaV_4S_8-1 and 177 K in GaV_4S_8-2 as shown in figure 3. From the slope of log ρ vs. $(1/T)^{1/4}$, the value of T_0 is found to be large in GaV_4S_8-2 compared to GaV_4S_8-1. Using the standard value of $c_3 = 2.436$ in T_0 expression, $\alpha/N^{1/3}$ is calculated and average α^{-1} is estimated to be small in GaV_4S_8-2 compared to GaV_4S_8-1 at a constant density of V_4-cluster. As the Bohr radii are different in both the compounds, the average bandwidth per V_4-cluster at constant density of V_4S_4 is calculated using the value of T_c and $\alpha/N^{1/3}$

Table 1. Low-temperature parameters calculated from DC resistivity.

Compounds	GaV_4S_8-1	GaV_4S_8-2
ρ (300 K)	4.0Ω cm	4.0 Ω cm
ε_3 (320–600 K)	0.23 eV	0.23 eV
ε_3 (300 K)	0.18 eV	0.18 eV
ε_3 (170 K)	0.05 eV	0.06 eV
T_0	0.51×10^8 K	0.68×10^8 K
T_c	170 K	177 K
$\alpha/N^{1/3}$	5.0	5.52
Γ	0.34 eV	0.37 eV

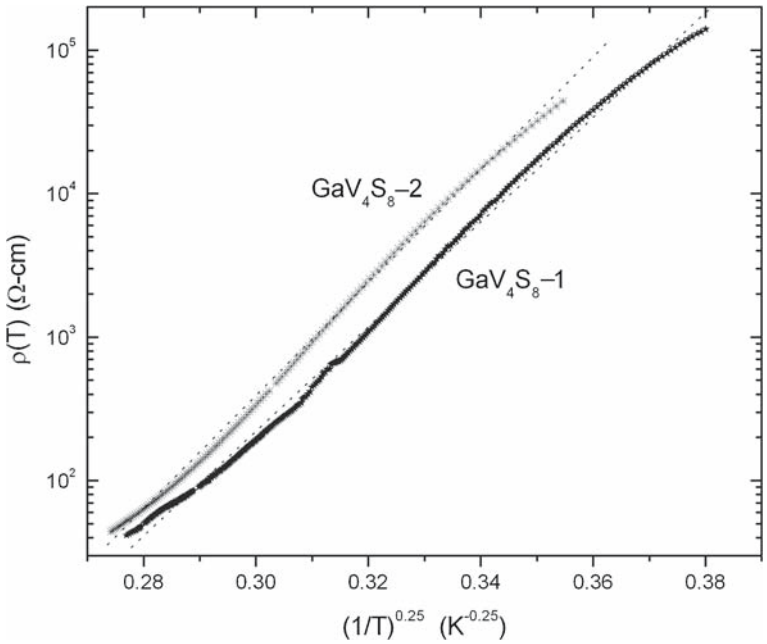

Figure 3. Mott's law, $\log \rho$ vs. $(1/T)^{1/4}$ well fitted in the non-Arrhenius region of GaV_4S_8-1 and GaV_4S_8-2.

from the expression of rectangular band of width 2Γ in which Mott's law holds for $E_{\max} \leq \Gamma$, where T_c is the upper limit of temperature for Mott's law.

$$k_B T_c = \left(\frac{\Gamma}{c_3}\right)^{4/3} \frac{1}{\alpha/N^{1/3}}. \tag{5}$$

From eq. (5), the bandwidths per cluster (Γ) are calculated to be ~0.342 and ~0.374 eV in GaV_4S_8-1 and GaV_4S_8-2, respectively indicating that the Bohr radius α^{-1} in GaV_4S_8-2 is small compared to GaV_4S_8-1.

Below 60 K. On cooling, there is a sharp downward jump followed by a nearly linear $\log\rho$ vs. $1/T$ dependence in the low-temperature region of 45 K in GaV_4S_8-1 and 43 K in GaV_4S_8-2 accompanied by structural phase transformation – cubic to rhombohedral as shown in figure 2. This phase transformation reduces the intercluster site distance as a result of which a sharp downward jump in resistivity is observed [9]. The GaV_4S_8-2, which was re-annealed at a lower temperature and which is expected to be having a better crystalline order, gave not only a sharper transition albeit at a lower temperature but also showed different temperature dependence in resistivity behaviour in the temperature range of 60–260 K.

3.3 *Magnetoresistance*

The temperature dependence of resistance with magnetic field $H = 6$T applied perpendicular to the flow of current is measured on GaV_4S_8-2 in the temperature range of 30–100 K

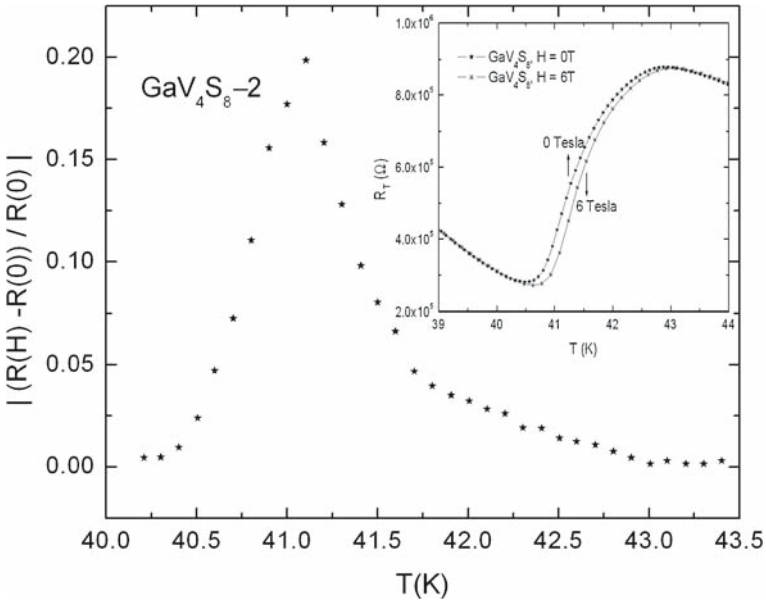

Figure 4. Magnitude of magnetoresistance vs. temperature below 43 K in GaV_4S_8-2. Inset figure shows the resistance in the magnetic field $H = 0$ T and 6 T in GaV_4S_8-2.

and plotted with zero magnetic field resistance around the phase transformation temperature i.e., 43 K as shown in figure 4 (inset). It is clearly shown in figure 4 (inset) that the resistance with field and without field are significantly different from each other within the temperature range of 40–43 K and beyond this temperature, both have identical values. The difference in resistance due to magnetic field, commonly known as magnetoresistance (MR), is found to be negative from the formula $\mathrm{MR} = \{R(H,T) - R(0,T)\}/R(0,T)$ and plotted in figure 4. Starting from the high-temperature range of 43 K, the magnitude of MR slowly increases with decreasing temperature. Below 42 K it rises very rapidly to attain a broad maximum around 41 K and then decreases nearly equal to 0 MR at 40.5 K. This is expected to be due to the effect of magnetic anomalies around 41 K as reported earlier [11,16]. In figure 4 (inset), the upturn in resistance with field and without field below 41 K is related to the semiconducting nature of GaV_4S_8-2 with rhombohedral symmetry having an activation energy of $\sim$0.04 eV calculated within our experimental limitations.

4. Conclusion

We have calculated some parameters like ε_3, α^{-1}, $\alpha/N^{1/3}$ and Γ using percolation theory in DC conductivity on two annealed compounds GaV_4S_8-1 and GaV_4S_8-2. Above 300 K, the average Bohr radius of the V_4-cluster in both the compounds is found to be the same irrespective of their crystal disorder. On cooling below 300 K, a decrease in activation energy is expected due to the increase in separation between the clusters which are significantly different for GaV_4S_8-1 and GaV_4S_8-2 and which provide the information

about decrease in Bohr radius. However, the rate of decrease in the average size of V_4-cluster/Bohr radius below 260 K on good crystalline compound, GaV_4S_8-2, is faster than GaV_4S_8-1. This statement is strongly supported by the calculated bandwidth Γ per cluster in GaV_4S_8 ($\sim$0.342 eV in GaV_4S_8-1 and $\sim$0.374 eV in GaV_4S_8-2). In GaV_4S_8-1, the resistance for the current flow is less because of the large cluster size/Bohr radius and gives better conductivity compared to GaV_4S_8-2. In other words, the cluster size decreases faster in GaV_4S_8-2, which is expected to have better crystalline order, than the lower crystalline order compounds below 260 K. Besides this, the negative MR found around 41 K in GaV_4S_8-2 is associated with the structural transition from cubic to rhombohedral expected due to the magnetic anomalies.

Acknowledgement

One of the authors (S Hansda) acknowledges UGC, New Delhi, India for the financial support through Rajiv Gandhi National fellowship to carry out this work.

References

[1] J M Vandenberg and D Brasen, *J. Solid State Chem.* **14**, 203 (1975)
[2] A K Rastogi, *Current trends in the Phys. Mater.* (World Scientific, Singapore, 1987) p. 316
[3] A R West, *Solid state chemistry and its application* (Reprint by Wiley India (P) Ltd., New Delhi, 2007) p. 569
[4] H Haeuseler, S Reil and E Elitok, *Int. J. Inorg. Mater.* **3**, 409 (2001)
[5] H Muller, W Kockelmann and D Johrendt, *Chem. Mater.* **18**, 2174 (2006)
[6] Y Sahoo and A K Rastogi, *J. Phys.: Condens. Matter* **5**, 5953 (1993)
[7] Y Sahoo and A K Rastogi, *J. Phys. Chem. Solids* **57**, 467 (1996)
[8] Y Sahoo and A K Rastogi, *Physica B* **215**, 233 (1995)
[9] R Pocha, D Johrendt and R Pottgen, *Chem. Mater.* **12**, 2882 (2000)
[10] H Nakamura, H Chudo and M Shiga, *J. Phys.: Condens. Matter* **17**, 6015 (2005)
[11] D Brasen, J M Vandenberg, M Robbins, R H Willens, W A Reed, R C Sherwood and X J Pinder, *J. Solid State Chem.* **13**, 298 (1975)
[12] C S Yadav, A K Nigam and A K Rastogi, *Physica B* **403**, 1474 (2008)
[13] A Miller and B Abrahams, *Phys. Rev.* **120**, 745 (1960)
[14] G E Pike and C H Seager, *Phys. Rev. B* **10**, 1421 (1974)
[15] M Pollak and M L Knotek, *J. Non-Crystall. Solids* **32**, 141 (1979)
[16] N Shanti and D D Sarma, *J. Solid State Chem.* **184**, 143 (1999)